ELSEVIER

Polymer 41 (2000) 8813–8823

polymer

www.elsevier.nl/locate/polymer

# Some aspects of the crystallization of ethylene copolymers

J.R. Isasi[a,1], J.A. Haigh[a], J.T. Graham[a,2], L. Mandelkern[a,*], R.G. Alamo[b]

[a]*Department of Chemistry and Institute of Molecular Biophysics, Florida State University, Tallahassee, FL 32306-4380, USA*
[b]*Department of Chemical Engineering, College of Engineering, Florida Agricultural and Mechanical University and Florida State University, 2525 Pottsdamer Street, Tallahassee, FL 32310-6046, USA*

Dedicated to the memory of Prof. A. Keller in honor of his contributions to polymer science.

Received 4 October 1999; received in revised form 10 February 2000; accepted 19 February 2000

**Abstract**

This report presents a continuation of studies from these laboratories that have been concerned with the crystallization behavior of ethylene copolymers. More specifically a comparison is made between the thermodynamic properties of ethylene–norbornene copolymers with those of the 1-alkene copolymers. In addition a detailed comparison is made of the thermodynamic, tensile, morphological and structural properties and the overall crystallization kinetics between the ethylene–1-alkene copolymers that do or do not contain small concentrations of long-chain branches. Except for the crystallization kinetics, the crystallization properties have been found to be essentially the same for both types of copolymers. A correlation has also been developed between the lamellar and supermolecular structures, the chemical nature of the comonomer and its concentration. Supermolecular structures range from spherulitic to micellar, depending on both comonomer type and concentration. Analysis of the overall crystallization kinetics demonstrates that the interfacial free energies that govern nucleation are independent of the lamellar and superstructures that evolve. 

*Keywords*: Copolymers; Norbornene; Crystallization kinetics

## 1. Introduction and background

Investigations on the crystallization of ethylene copolymers have accelerated in the recent years with the advent of the metallocene type catalysts. These catalysts yield polymers that have most probable molecular weight and relatively narrow composition distributions. In this paper, we elaborate on the previous reports from our laboratory that dealt with the crystallization behavior of the ethylene–1-alkene copolymers [1–4]. New results that have been obtained with ethylene–norbornene copolymers will also be introduced. The previous work was limited to copolymers that did not contain long chain branches [1–3]. It is, therefore, of interest to compare the crystallization properties of the ethylene–1-alkene copolymers that contain small concentrations of long chain branches [5,6] with those that do not. More specifically, we shall examine melting temperatures, crystallinity levels determined by different methods, crystallization kinetics, some aspects of mechanical properties and the relation between the lamellar and supermolecular structures in terms of composition and the chemical nature of the comonomer of both copolymer types.

In designing these, as well as other studies, certain basic concepts have to be kept in mind that are unique to random copolymers. A major factor that needs to be recognized is that both the molecular weight and composition are independent variables [4]. This is a very fundamental principle. Therefore, when properly comparing properties both the molecular weight and copolymer composition need to be matched as closely as possible. We shall follow this protocol in the present work. The properties that are observed will depend on the temperature-time path taken from the melt [7]. This is particularly true after isothermal crystallization. To avoid complications in interpretation due to the variety of crystallization pathways that are available, we have limited our studies to two crystallization modes. One involves rapid cooling (quenching) from the melt. The other involves isothermal crystallization without cooling subsequent to initiating the fusion process. In this paper, attention will be given to the former process. The important results obtained when the latter isothermal crystallization mode is followed will be reported subsequently [8]. When

* Corresponding author. Tel.: +1-85-644-2054; fax: +1-85-644-1701.
*E-mail address:* mandelk@val.sb.fsu.edu (L. Mandelkern).
[1] Present address: Departamento de Quimica y Edafologia, Facultad de Ciencias, Universidad de Navarra, c/Irunlarrea s/n, 31080 Pamplona, Spain.
[2] Present address: Department of Chemistry, University of Florida, Gainesville, FL, USA.

0032-3861/00/$ - see front matter 
PII: S0032-3861(00)00224-X

Table 1
Molecular characteristics of copolymers (EB-Ethylene butene; EO-Ethylene octene)

| Designation | $M_w$ | $M_w/M_n$ | $1 - X_A \times 100$ | $I_{10}/I_2$ [a] |
|---|---|---|---|---|
| (A) Ethylene–norbornene | | | | |
| A | 80,800 | 2.3 | 1.0 | |
| B | 86,300 | 2.1 | 1.6 | |
| C | 111,300 | 2.4 | 2.1 | |
| D | 111,900 | 2.4 | 2.5 | |
| E | 97,400 | 2.5 | 3.6 | |
| (B) Ethylene–1-alkenes (long branches) | | | | |
| EB-A | 100,800 | 2.0 | 1.4 | 7.56 |
| EO-B | 121,700 | 2.0 | 6.5 | 7.26 |
| EO-C | 142,800 | 2.1 | 6.3 | 7.75 |
| EO-D | 103,300 | 2.3 | 4.1 | 8.50 |
| EO-E | 91,600 | 2.3 | 2.5 | 8.12 |
| EO-F | 87,800 | 2.3 | 1.95 | 9.58 |
| EO-G | 84,500 | 2.2 | 1.5 | 9.88 |
| EO-H | 71,200 | 2.10 | 0.35 | 7.11 |

[a] This ratio is described in the text.

studying the crystallization of copolymers, it is necessary a priori to establish whether or not the crystalline phase remains pure. When the comonomer enters the lattice it has to be established further whether it does so on an equilibrium basis or as a true defect. This complex problem has been simplified for the copolymers studied here since it has been shown that except for the methyl groups of 1-propene, other comonomers of the 1-alkenes do not enter the lattice [4,9].

Composition and molecular weight distributions also effect the crystallization behavior of random copolymers of ethylene. Consequently our studies have been limited to composition and molecular weight fractions of Ziegler–Natta type copolymers, metallocene catalyzed copolymers and hydrogenated poly(butadienes). The latter are equivalent to random ethylene–butene copolymers of very narrow molecular weight ($M_w/M_n \simeq 1.1 - 1.2$) and composition distributions. The source and catalyst type has been reported already [1–3]. The ethylene–norbornene copolymer falls in the same category. The long-chain branched copolymers were received from the Dow Chemical Co. and are similar to those described by others [5,6].

## 2. Experimental

The molecular characteristics of the new copolymers studied here are given in Table 1. Table 1 gives the molecular weight and composition of the ethylene–norbornene copolymers in terms of the mole percent (mol%) comonomer incorporated into the chain. Table 1 gives the same characteristics for the 1-alkene copolymers that contain small concentrations of long-chain branches [5,6]. The last column in Table 1, $I_{10}/I_2$ is the ratio of the melt flow index at 190°C at loads of 10 and 2.16 kg, respectively. This ratio reflects the number of long-chain branches [5,6]. A value of 6 indicates the virtual absence of long branches. The characteristics of the copolymers that are devoid of long-chain branches, and with which the comparisons are being made, have already been described [1–3].

The experimental techniques employed in the present work have been described in great detail in the previous reports from these laboratories [1–3] and need not be repeated here. In brief, the thermal analysis and differential scanning calorimetry (DSC) were carried out using a Perkin–Elmer DSC2 calibrated with indium. The measurement of the enthalpy of fusion from the standard DSC endotherm was carried out by calculating the area in the temperature interval between −5°C (±5°C depending on the copolymer) and the melting point. The variation of the heat capacity of the liquid polymer with temperature was approximated to a straight line. The measured enthalpies of fusion were converted to the degree of crystallinity, $(1 - \lambda)_{\Delta H}$, by taking the enthalpy of fusion of the perfect macroscopic crystal to be 290 J/g (69 cal/g) [10]. The crystallization kinetics of the metallocene copolymers were measured by DSC using the endothermic method described previously [11]. To obtain reproducible results from the crystallization kinetics, it was necessary that the polymers be purified and residual catalysts removed. To accomplish this, the copolymers used in the kinetic studies were pressed into thin films and cut into small pieces. They were then dissolved in *p*-xylene at about 100°C at a concentration of about 0.2 g/ml. After complete dissolution, the solution was cooled to room temperature and the copolymers were precipitated by the addition of cold methanol. The copolymer precipitates were collected by filtration, washed several times with methanol and dried under vacuum for 24 h.

The sample densities were measured at 23°C in a 2-propanol–water density gradient column calibrated with standard glass floats [1]. The density values were converted to the degree of crystallinity, $(1 - \lambda)_d$, by the relationship given by Chiang and Flory [12].

The force–elongation curves were obtained in an apparatus that has been described previously. Deformation properties can be determined using as little as 100 mg of the sample [13].

The small-angle light scattering patterns (SALS) were obtained using a photometer developed by Stein, and its use has been described previously [14]. The description and designation of the supermolecular structures observed has been defined previously also [14,15]. The transmission electron micrographs (TEM), were obtained utilizing the Kanig method [16] as has been defined [17,18]. This technique was applied to the study of hydrogenated poly(butadienes) as well as other random ethylene copolymers [19].

As was indicated above, we have adopted deliberately a rapid crystallization procedure to allow for a rational comparison to be made between the different copolymers. Therefore, prior to study, the samples were initially crystallized by quenching from the melt into a mixture of isopropyl alcohol and dry ice, at −78°C.

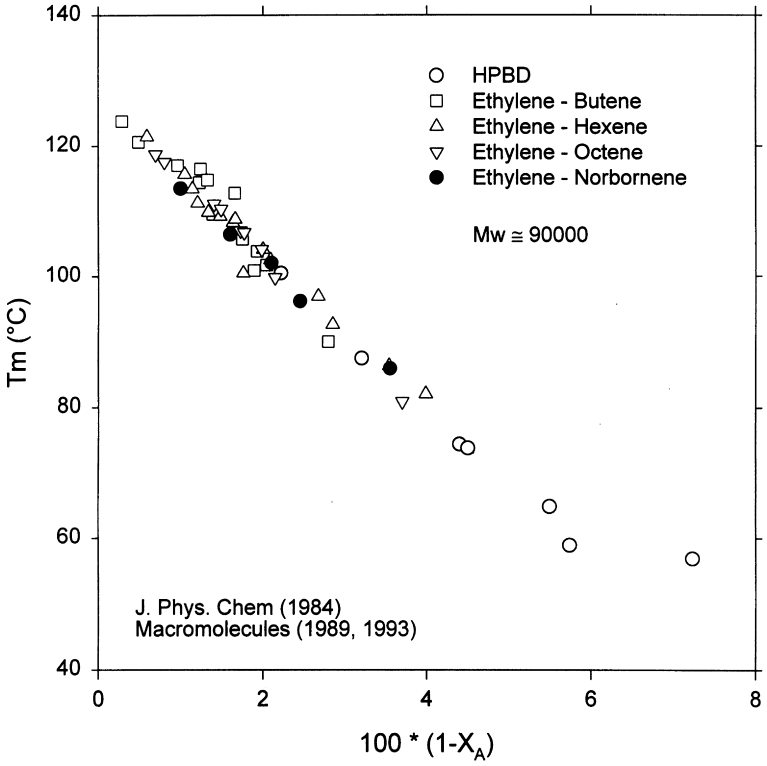


Fig. 1. Plot of observed melting temperature $T_m$ against mol% of structural irregularities in chain. Comonomers indicated. HPBD stand for hydrogenated poly(butadiene).

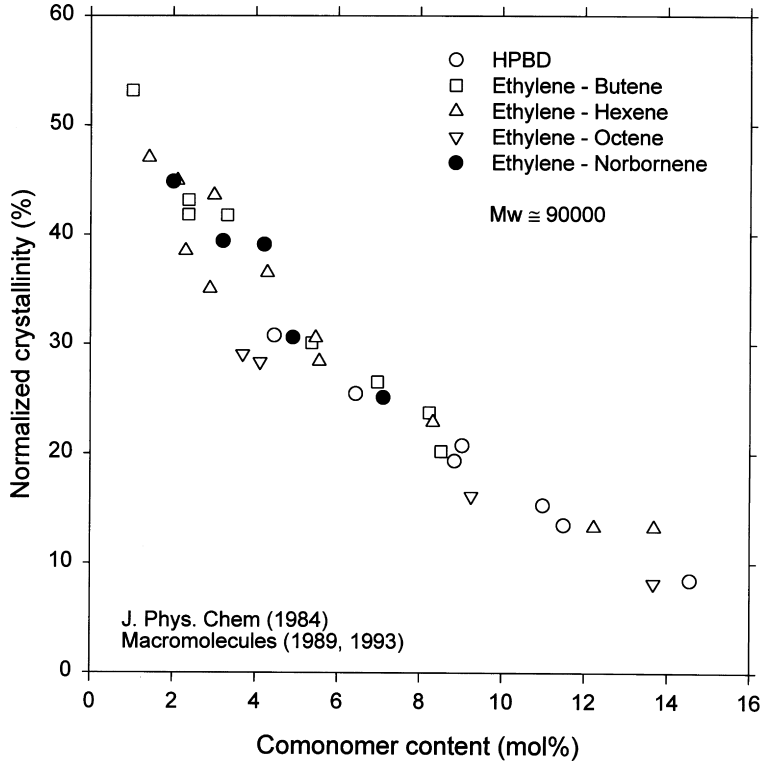


Fig. 2. Plot of degree of crystallinity, $(1-\lambda)_{\Delta H}$, against mol% of structural irregularities. Comonomers indicated. HPBD stands for hydrogenated poly (butadiene).

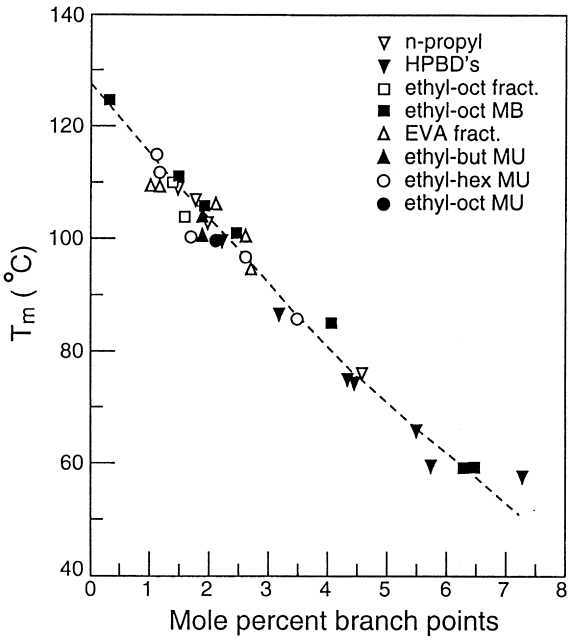


Fig. 3. Plot of observed melting temperature, $T_m$, against mol% branch points. HPBD stands for hydrogenated poly(butadiene). MB represents metallocene catalyzed copolymer with long-chain branches; MU represents metallocene catalyzed copolymers without long-chain branches.

## 3. Results and discussion

We consider first the thermodynamic behavior of the ethylene–norbornene copolymers and compare their properties with those reported previously for the ethylene–1-alkenes and other random ethylene copolymers. The observed melting temperature, $T_m$, is plotted against the mol% of structural irregularities in Fig. 1 for the different copolymer types. In this plot $T_m$ has been taken as the peak melting temperature in the thermograms. As has been pointed out properly, the final melting temperature should be used [20]. However, the difference between the two melting temperatures is small so that the use of the maximum does not sensibly alter the plot and the conclusions reached. As expected, there is a smooth monotonic decrease in the melting temperature with the comonomer concentration of each copolymer. We see from this plot that the observed melting temperatures of the alkene copolymers are independent of the chemical nature of the branch or co-unit. This is expected, since for a random copolymer, whose crystalline phase remains pure, the depression in the melting temperature only depends on the mol% of non-crystallizing units and not on their chemical nature. These results for the alkene copolymers were initially reported about 16 years

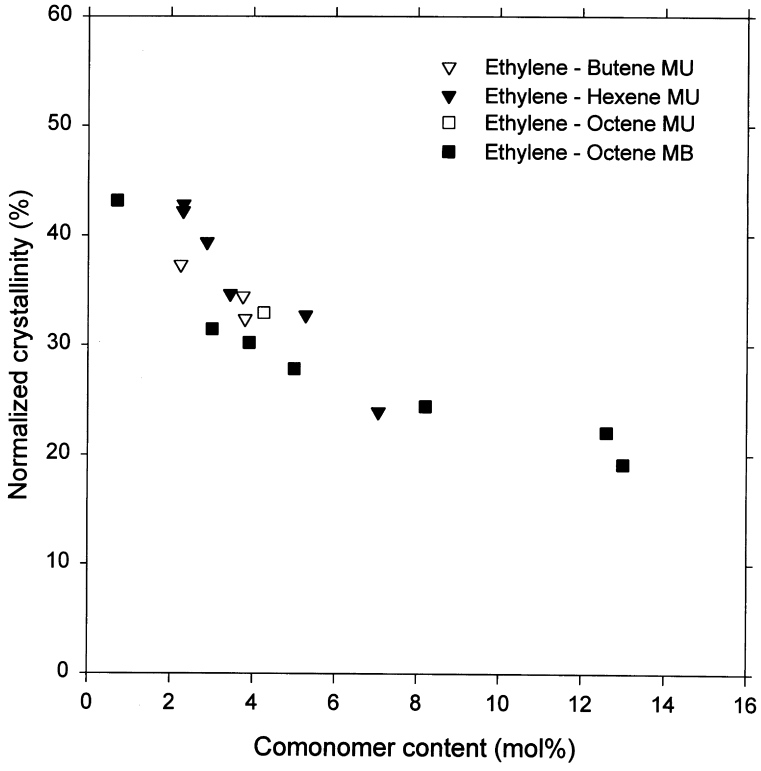


Fig. 4. Plot of degree of crystallinity $(1-\lambda)_{\Delta H}$ against mol% branch points of metallocene crystallized copolymers. Copolymer with long-chain branches, MB; without long-chain branches MU.

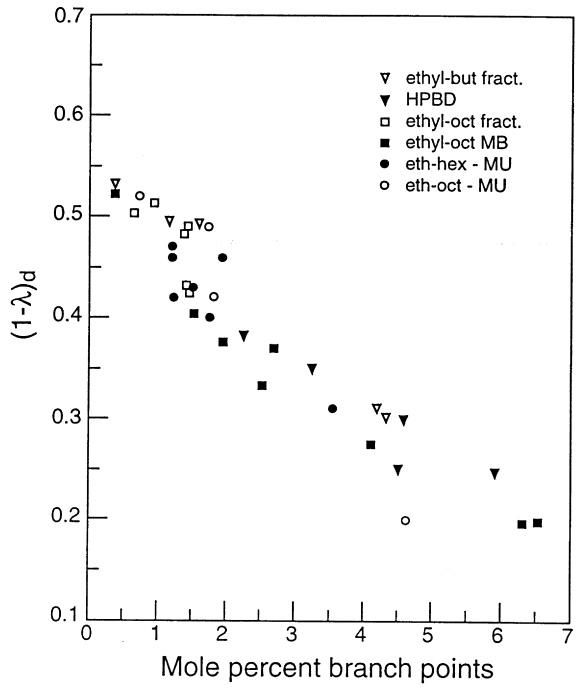


Fig. 5. Plot of degree of crystallinity, $(1-\lambda)_d$, against mol% branch points for ethylene–1-alkene copolymers. MB represents metallocene catalyzed copolymers with long-chain branches; MU represents metallocene catalysed copolymers without long-chain branches.

ago. They have been confirmed in a recent report [21]. Of particular interest are the results for the norbornene copolymers. Surprisingly, the melting temperature–composition relation for this set of copolymers is identical with those of the 1-alkenes. One might have expected that the insertion of the ring in the chain would affect the chain conformation and thus the entropy of fusion. However, in the range of copolymer compositions studied here there is no perceptible influence of the ring structure on the observed melting temperature. Based on the equilibrium theory the melting temperature will depend on the sequence propagation probability. However, for the rapid crystallization procedures used here, the resulting thin crystallites, and the interfacial free energy associated with the basal plane, will dominate the melting. However, we have found that even after isothermal crystallization at elevated temperatures, the melting temperatures of the norbornene copolymers are the same as those for the 1-alkenes [8].

Fig. 2 is a plot of the crystallinity, normalized for the mass fraction of ethylene, against the mol% of comonomers for the same copolymers. The crystallinity levels for both types of copolymers decrease monotonically with the comonomer concentration. The results for the 1-alkene copolymers are the same at each composition, independent of the length of the short chain branch. These results have also been confirmed in a recent report [21]. The $(1-\lambda)_{\Delta H}$ values

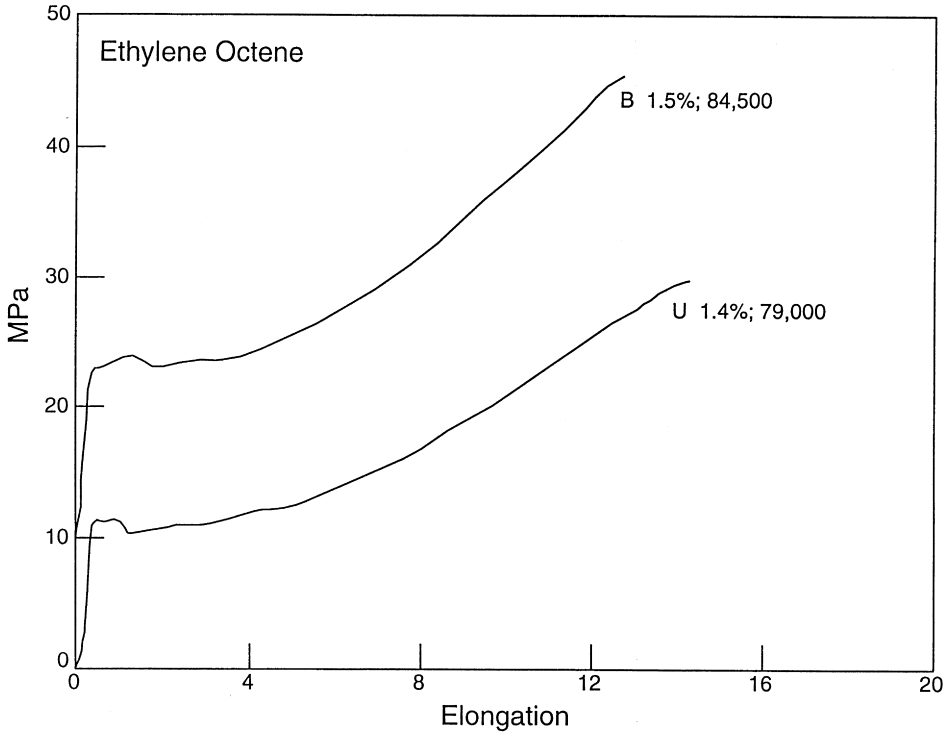


Fig. 6. Force–elongation curves of a matched pair of ethylene–octene metallocene catalysed copolymers. Copolymer B, ($M_w = 84,500$ 1.5 mol% branch points) contains long-chain branches. Copolymer U ($M_w = 79,000$, 1.4 mol% branch points) does not contain long-chain branches.

Table 2
Comparison of tensile properties of ethylene octenes

| Polymer | $M_w \times 10^{-3}$ | Mole % branch pts. | $(1-\lambda)_{\Delta H}$ | $T_m$°C | Yield stress | Ult. ten. stress | $\lambda_B$ |
|---|---|---|---|---|---|---|---|
| Branched | 84.5 | 1.5 | 0.32 | 111.1 | 10.51 | 27.34 | 6.5 |
| Unbranched | 79.0 | 1.4 | 0.27 | 110.4 | 10.80 | 27.54 | 6.5 |

for the norbornene copolymers follow the same pattern as the 1-alkenes. We can conclude that the thermal properties of ethylene–norbornene copolymers are virtually identical to those reported earlier for ethylene–1-alkene copolymers for this mode of crystallization.

In comparing the long and non-long chain branched ethylene 1-alkene metallocene catalyzed copolymers, we first consider thermodynamic properties. Fig. 3 is a plot of the melting temperature against mol% branch points for the fractions and both types of metallocene copolymers. The metallocene copolymers are indicated by M followed by B for long branched and U for non-branched. All of the observed melting points can be represented by a common curve. There is no discernable difference between the two types of copolymers.

The normalized level of crystallinity, as obtained from the enthalpy of fusion, is plotted against the mol% comonomer in Fig. 4 for the long-chain branched and unbranched copolymers. Within the experimental error one can not discriminate between the two types of copolymers. A similar conclusion is reached when the level of crystallinity, as calculated from the density, is plotted against the mol% of branch points as shown in Fig. 5. These results, showing that there is no difference in thermodynamic properties between the copolymers, with or without long-chain branches, differ from those reported by Bensason et al [22]. The long-chain branched polymers in both studies were from the same source. The reason(s) for the difference between the two works is not clear. In both studies the same constants were used to determine the levels of crystallinity and the same type of density gradient column was used. The work reported here and earlier were metallocene type copolymers. Thus, the difference in the two works can not be attributed to polydispersity effects.

A comparison has been made also of tensile properties by means of force–elongation measurements. A set of force–elongation curves are shown in Fig. 6 for a matched pair of ethylene–octene copolymers, one that has long-chain branches (B) and one without (U). The molecular weights and compositions of the two copolymers have been closely matched. In this figure, the two curves have been displaced by 10 MPa for clarity. Except for minor differences in the yield region, the shapes of the two curves are very similar to one another. This similarity is emphasized by the data in Table 2 where the values of the key tensile properties are compared. Within experimental error, the yield stress, ultimate tensile stress and draw ratio at break, $\lambda_B$, are identical with one another. One can conclude that the introduction of long-chain branches into the chain does not affect the tensile properties of the rapidly crystallized copolymers.

The overall crystallization kinetics of two pairs of matched ethylene–octene copolymers were studied by DSC using the endothermic method. As mentioned in the

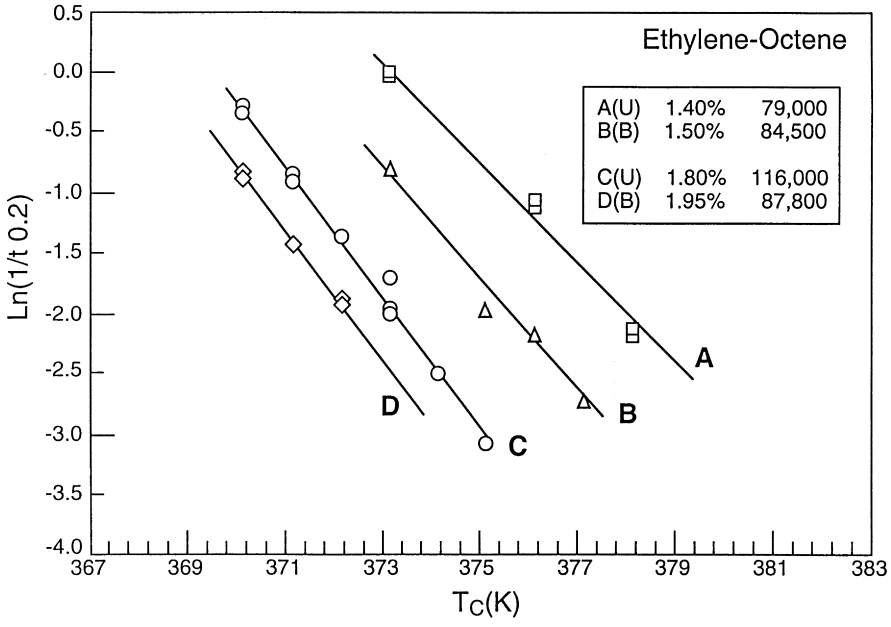


Fig. 7. Plot of ln of crystallization rate ($1/\tau_{0.2}$) against crystallization temperature for indicated matched pairs of ethylene–octene copolymers. B represents copolymers with long-branches; U represents copolymers without long branches.

experimental part, the polymers were purified from residual catalyst before the crystallization kinetics were carried out. The results are shown in Fig. 7. Here the crystallization rate, expressed as $\ln(1/\tau_{0.2})$, where $\tau_{0.2}$ is the time for 20% of the transformation to be completed, is plotted against the crystallization temperature $T_c$. The molecular weights and mol% of branch points are indicated in the figure. The temperature coefficients of the crystallization rates of the copolymers in each pair are close to one another, as they are between pairs. When analysed according to nucleation theory the products of the interfacial free energies $\sigma_{en}\sigma_{un}$ are close to one another, independent of copolymer composition and whether or not long-chain branches are incorporated into the chain. There is, however, a major difference in the crystallization rate that depends on the presence or absence of long-chain branches. At a given crystallization temperature, the copolymer that contains the long-chain branches crystallizes at an appreciably slower rate, in each matched pair. This is a consequence of the influence of the long-chain branches on the transport term that appears in the general expression that describes crystallization kinetics [23]. A similar effect of long-chain branches on the crystallization kinetics has been observed in three-arm star polymers [24]. Among all of the solid state properties of copolymers that have been studied here, only the crystallization kinetics are influenced by the presence of long-chain branches. The other properties studied, such as thermal properties, crystallinity levels, and tensile properties are indistinguishable between the two copolymer types.

One can also compare the lamellar and supermolecular structures of the long-chain branched and unbranched ethylene–1-alkene copolymers. Much of the pertinent data has been reported already in the literature by several research groups [5,19,22,25]. In addition to the comparison, the data themselves contain important structural information that has applicability to other problems. A set of TEM for a series of hydrogenated poly(butadienes), whose composition varied but have a fixed molecular weight, $M_w = 108,000$ g/mol, have been published [19]. The weight to number average ratio, of what are ethylene–butene copolymers, is 1.1–1.2 and the composition distribution is extremely narrow as indicated by their TREF analysis. A copolymer with 2.2 mol% branch points still yields a lamellar type structure. However, the lamellae are not as well developed as those found in the corresponding homopolymers and they are not stacked in a regular array. Thus, at this composition the lamellar morphology is quite different from that expected and observed in homopolymers. For a hydrogenated poly(butadiene) with 3.2 mol% branch points, lamellae are still observed. However, at this composition, they are small in the lateral direction and curved. For a 4.5 mol% copolymer of this kind the crystallites are very small and non-lamellar although the crystallinity is still in the range 10–15%. Thus, as the co-unit is increased there is a significant deterioration of the lamellar structure. A composition is reached, between 3.2 and 4.5 mol% branch points, where crystallization is observed without the association of any lamellar structures. The fact that even at low co-unit content the lamellae are not well developed, presents problems if when properties are analysed it is assumed that the lamellae are well developed, stacked in a regular array and connected one to the other by disordered regions.

A comparison between the electron micrograph results and the SALS patterns of the same copolymers allows for a correlation to be made between lamellar and supermolecular structures. A morphological map for the hydrogenated poly(butadienes), and ethylene–butene, non long-chain branched copolymers has been reported [25]. Copolymers with $M \simeq 100,000$ g/mol, which correspond to the electron micrographs, are devoid of spherulitic, or any supermolecular structure, when the mol% of branch points is greater than 2%.

A similar correlation has been reported by Minick et al [5], and Bensason et al [22] for ethylene–octene copolymers that contained long-chain branches. For these copolymers, the pattern of lamellar degradation and the eventual disappearance of spherulitic structure is very similar to that found with the hydrogenated poly(butadienes). A major difference, however, is that with the hexyl branched copolymers the disappearance of lamellar structure occurs at a lower short-chain branch content than was found for the ethyl branched ones. It is not surprising that the longer hexyl branch retards the perpetuation of the lamellar crystallites, since the probability of the return of a sequence to the crystallite of origin is reduced.

The correlation between lamellar structure, as described by electron microscopy, and the supermolecular structure deduced from SALS or optical microscopy has also been found for ethylene–vinyl acetate copolymers [26]. Low density polyethylene, which contains a significant concentration of long-chain branches relative to the metallocene copolymers, shows a similar relation between the lamellar and supermolecular structure. Electron microscopy studies have shown that as the concentration of long-chain branches increases the lamellar character of the crystallites progressively deteriorates [27,28]. Concomitantly, the superstructure becomes less well-defined and eventually the supermolecular structure is no longer observed [29]. A similar correlation scan be made for linear polyethylene fractions. Thin section electron microscopy studies have shown that there are systematic variations in the lamellar structure with molecular weight that correlate quite well with the changes in the supermolecular structure [26,30]. At low to moderate molecular weights, well-developed lamellae that are straight and long are observed, while well-organized supermolecular structures are formed. With an increase in the molecular weight the lamellae become curved and short as the spherulite structure continually deteriorates. At high molecular weights, $\sim 10^6$ and greater, the lamellae become highly segmented and there is no evidence of any organized superstructure. Only randomly arranged, segmented lamellae are observed. It can be concluded that, for the polyethylenes at least, the key factor in determining the supermolecular

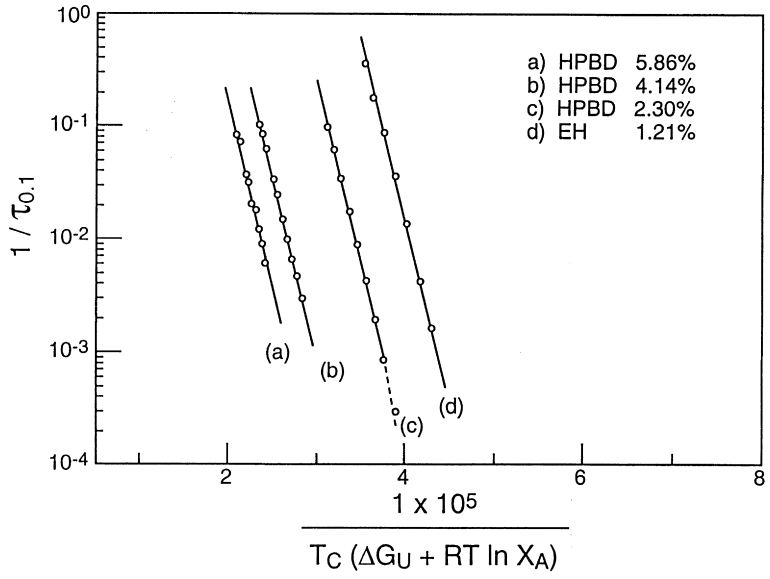


Fig. 8. Plot of crystallization rate ($1/\tau_{0.1}$) against nucleation temperature functions for indicated copolymers.

structure, or the lack thereof, is how well the lamellar crystallites are developed. Therefore, in analysing and interpreting the different superstructures that evolve, focus should be given to the basic nature of the lamellar crystallites.

Since it has been shown that a range in morphological structures from spherulitic to micellar can be formed by varying the copolymer composition, one has an unique opportunity to ascertain what influence, if any, such structures have on the overall crystallization kinetics. Such studies with the hydrogenated poly(butadienes) have shown that there is a very marked negative temperature coefficient to the process, indicating nucleation controlled crystallization [31]. To analyse the kinetics, a specific type of nucleation has to be assumed. For illustrative purposes, we have taken a Gibbs type coherent, unimolecular nucleus as being operative. The major conclusion that is reached does not depend on the particular nucleation process selected for the analysis. The same results are obtained irrespective of whether homogeneous, or various types of heterogeneous nucleation processes were chosen for the analysis. The purpose here is not to establish the specific type of nucleation that is involved but rather to learn whether the nucleation parameters, i.e. the appropriate interfacial free energies depend on the morphological structures that eventually evolve.

We define the overall crystallization rate here as $1/\tau_{0.1}$, where $\tau_{0.1}$ represents the time for 10% of the transformation to be completed. In standard fashion $\ln(1/\tau_{0.1})$ is taken to be proportional to $\Delta G^*$, the critical free energy of forming a nucleus. For the type of nucleus that is being assumed [31]

$$\Delta G^* = 4\sigma_{en}\sigma_{un}/(\Delta G_u + RT \ln X_A). \quad (1)$$

Here $\sigma_{en}$ and $\sigma_{un}$ are the interfacial free energies of the surfaces that are normal and parallel to the chain axes, respectively. These interfacial free energies are not, and should not, be a priori identified with the corresponding surfaces of the mature crystallites that eventually evolve from the nucleus. The quantity $\Delta G_u$ is the free energy of fusion per repeating unit of the corresponding homopolymer and $X_A$ the mole fraction of crystallizable units. Therefore, according to nucleation theory a plot of $\ln(1/\tau_{0.1})$ against $1/T_C(\Delta G_u + RT \ln X_A)$ should be linear. The slope is directly related to the product of the interfacial free energies for nucleation. Such a plot is given in Fig. 8 for the hydrogenated poly(butadienes) of varying compositions and an ethylene–hexene copolymer (EH) that has a lower small-branch concentration. A family of straight lines results, that are displaced according to composition, reflecting the changing time scale. The values of the slopes are given in Table 3 and are constant within experimental error. Thus, it can be concluded that the product $\sigma_{en}\sigma_{un}$ is independent of the superstructures that eventually evolve and on the perfection of the lamellar crystallites. The same values for the interfacial free energies are found irrespective of whether or not reasonably well-developed lamellae are developed at all. It is assumed that the lamellar structure in this range of crystallization temperature are the same as in slow cooled samples.

The consequence of the analysis of these crystallization kinetics is profound. It is demonstrated that it is not required, or necessary, to relate the chain conformation within the nucleus to that within the mature crystallite. The nucleus is a relatively small entity as compared to the

Table 3
Comparison of slopes (proportional to $\sigma_{en}$ $\sigma_{un}$) from Fig. 8 $M_w \simeq 50,000$ g/mol

| Copolymer | Mole % branch pts. | $10^{-5}$ slope |
|---|---|---|
| EH | 1.21 | 7.63 |
| HPBD | 2.30 | 7.45 |
| HPBD | 4.14 | 7.59 |
| HPBD | 5.68 | 8.28 |

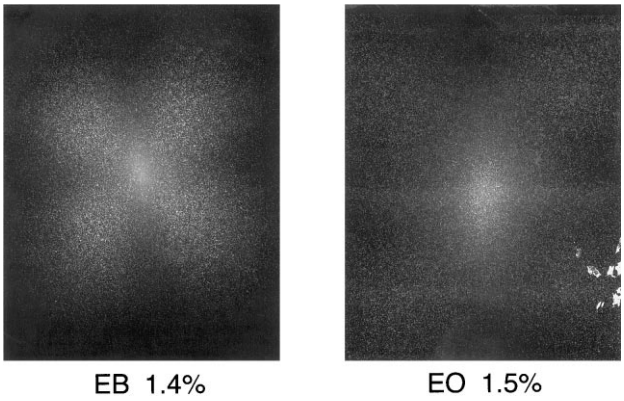


Fig. 9. SALS pattern, $H_V$, for long-chain branched copolymers. EB is for ethylene–butene $M_w = 100,800$ g/mol, 1.4 mol% branch points. EO is for ethylene–octene $M_w = 84,500$ g/mol, 1.5 mol% branch points.

crystallite. Their interfacial structures will be quite different. A similar conclusion was reached in analysing both the growth and overall crystallization rates of high molecular weight *n*-alkanes [32–34]. In these instances the same interfacial free energy for nucleation was involved irrespective of whether extended or folded chain crystallites were formed. Fractions of low molecular weight linear polyethylene show a similar behavior [35].

The influence of the chemical nature of the branches, (short and long) can also be analysed. As has been described above, a comparison of TEM has shown that the beginning of the dissipation of the lamellar structure begins at lower comonomer concentrations in the long-chain branched ethylene–octene copolymers as compared to ethylene–butene or hydrogenated poly(butadienes) that are devoid of the long branches. SALS patterns have shown that for copolymers without long-chain branches, at a given molecular weight, the ethylene–butenes display respectable spherulites, which deteriorated in the ethylene–hexenes and were not observed at all in ethylene–octene and ethylene–4-methyl pentene copolymers [25]. In particular, SALS patterns were presented in the molecular weight range of 70,000 g/mol and of 100,000 g/mol, at 1.1–1.2 mol% branch points that specifically highlighted these observations (see Ref. [25], figure 4). It has been since shown that spherulites are not observed in ethylene–norbornene copolymers with comparable molecular weights and comonomer composition [8]. Optical microscope observations show the same pattern in the supermolecular structures with different type co-units when the copolymers are crystallized at elevated temperature.

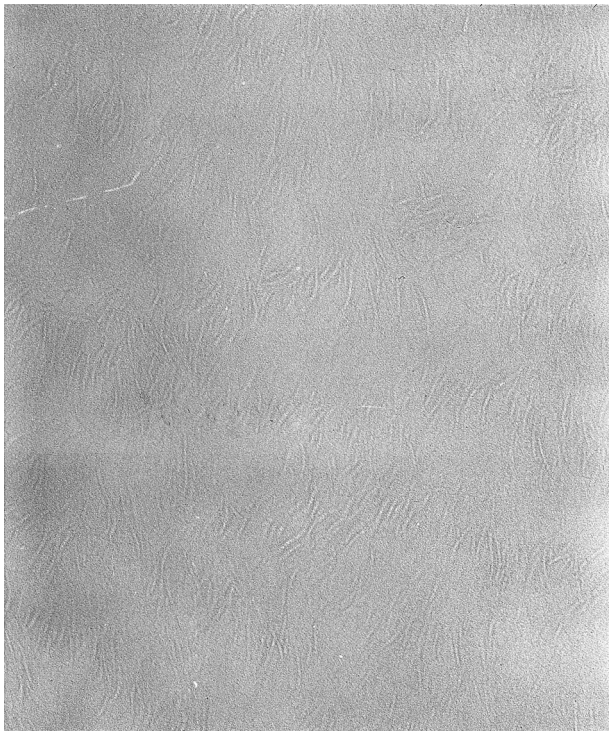

Fig. 10. TEM for an ethylene–butene copolymer without long-chain branches. $M_w = 71,000$ g/mol; 1.22 mol% branch points.

Fig. 11. TEM for an ethylene–hexene copolymer without long-chain branches. $M_w = 68,000$ g/mol; 1.14 mol% branch points.

Comparable SALS patterns for ethylene–butene and ethylene–octene copolymers that possess long-chain branches are illustrated in Fig. 9. These two copolymers have molecular weights of 100,800 g/mol and 84,500 g/mol and mol% of branch points of 1.4 and 1.5%, respectively. The pattern for the ethylene–butene copolymer gives direct evidence for a spherulitic type superstructure. On the other hand, the ethylene–octene pattern does not give any indication of a defined superstructure. Thus, the presence of long-chain branches does not minimize the influence of the

Fig. 12. TEM for an ethylene–octene copolymer without long-chain branches. $M_w = 79,000$ g/mol; 1.4 mol% branch points.

chemical nature and length of the short-chain branch on the superstructures that are formed.

If the premise that correlates the lamellar and supermolecular structures is correct then there should be changes in the lamellar structures between ethylene–butene, ethylene–hexene and the ethylene–octene copolymers. TEM for such a series of copolymers without long-chain branches, (the same as referred to above and illustrated in Ref. [25], figure 4), $M_w = 70,000$ g/mol, 1.1–1.4 mol% branch points are given in Figs. 10–12. Fig. 10, the ethylene–butene copolymer, shows distinct lamellae that are, however, curved and restricted in the lateral directions. The micrograph for ethylene–hexene (Fig. 11) shows much smaller lamellae but they are still discernable and profuse. The structures for ethylene–octene, as shown in the micrograph of Fig. 12, are quite different. Although the level of crystallinity is still the same, about 30%, the lamellae are now isolated and very sparse. Thus, the TEM are consistent with the SALS patterns. Similar constituted copolymers that have the same level of crystallinity, can develop very different supermolecular and lamellar structures.

In summary, the microscopic and SALS studies demonstrate a very strong correlation between the lamellar and supermolecular structures, for the 1-alkene copolymers, irrespective of whether or not they contain small concentrations of long-chain branches. There is also a strong influence of the length of the short chain branch on the lamellar structure and thus in turn on the superstructure.

## Acknowledgements

The TEM was carried out by Mr R. Würfel of the Institute für Physakalische Chemie, Johannes Gutenberg-Universitat, Mainz, Germany. We wish to acknowledge and thank him for the electron micrographs. Mr Adrian Little, a Chemical Engineering student in the NSF supported REU program, made significant contributions to this work. We also gratefully acknowledge support of this work by the National Science Foundation Polymer Program (DMR 94-19508).

## References

[1] Alamo R, Domszy R, Mandelkern L. J Phys Chem 1984;88:6587.
[2] Alamo RG, Mandelkern L. Macromolecules 1989;22:1273.
[3] Alamo RG, Viers BD, Mandelkern L. Macromolecules 1993;26:5740.
[4] Alamo RG, Mandelkern L. Thermochim Acta 1994;238:155.
[5] Minick J, Moet A, Hiltner A, Baer E, Chan SP. J Appl Polym Sci 1995;58:1371.
[6] Lai S. Knight GW. ANTEC 93 SPE Conference Proceedings, 1993. p. 1188.
[7] Mandelkern L, Glotin M, Benson RS. Macromolecules 1981;14:22.
[8] Haigh JA, Alamo RG, Mandelkern L. (in preparation).
[9] Richardson MJ, Flory PJ, Jackson JB. Polymer 1963;4:221.
[10] Alamo RG, Mandelkern L. In: Mark JE, editor. American Institute of Physics Handbook of Polymer Properties, 1996. 119pp.
[11] Galante MJ, Mandelkern L, Alamo RG, Lehtinen A, Paukkeri R. J Therm Anal 1996;47:913.
[12] Chiang R, Flory PJ. J Am Chem Soc 1961;83:2857.
[13] Peacock AJ, Mandelkern L. J Polym Sci, Polym Phys Ed 1990;28:1917.
[14] Maxfield J, Mandelkern L. Macromolecules 1977;10:1141.
[15] Mandelkern L. Organization of Macromolecules, in the Condensed Phase. In: Young DA, editor. Discussion Faraday Society, vol. 68, 1979. p. 310.
[16] Kanig G. Prog Colloid Polym Sci 1975;57:176.
[17] Voigt-Martin, IG, Mandelkern L. J Polym Sci, Polym Phys Ed 1981;19:1769.
[18] Voigt-Martin IG, Mandelkern L. J Polym Sci, Polym Phys Ed 1984;22:1901.
[19] Voigt-Martin IG, Alamo R, Mandelkern L. J Polym Sci, Polym Phys Ed 1986;24:1283.
[20] Crist B, Howard PR. Macromolecules 1999;32:3057.
[21] Alizadeh A, Richardson L, Xu J, McCartney S, Marand H, Cheung YW, Chum S. Macromolecules 1999;32:6221.
[22] Bensason S, Minick J, Moet A, Chum S, Hiltner A, Baer E. J Polym Sci, Part B: Polym Phys 1996;34:1301.
[23] Mandelkern L. Crystallization of polymer. New York: McGraw-Hill, 1964.
[24] Haigh JA, Nguyen C, Alamo RG, Mandelkern L. J Therm Anal 2000;59:435.
[25] Failla MD, Lucas JC, Mandelkern L. Macromolecules 1994;27:1334.
[26] Chowdhury F, Haigh JA, Mandelkern L, Alamo RG. Polym Bull 1998;41:463.
[27] Michler GH, Brauer E. Acta Polym 1983;34:533.
[28] Michler GH, Nanmann I. Morphology of polymers. In: Sedlacek B, editor. Berlin: Walter de Gruyter, 1986. p. 329.
[29] Mandelkern L, Maxfield J. J Polym Sci, Polym Phys Ed 1979;17:1913.

[30] Voigt-Martin IG, Fischer EW, Mandelkern L. J Polym Sci, Polym Phys Ed 1980;18:2347.
[31] Mandelkern L. Crystallization of polymer. New York: McGraw-Hill, 1964 p. 241 ff.
[32] Mandelkern L, Alamo RG, Haigh JA. Macromolecules 1998;31:765.
[33] Alamo RG, Mandelkern L, Stack GM, Kröhnke C, Wegner G. Macromolecules 1994;27:147.
[34] Stack GM, Mandelkern L, Kröhnke C, Wegner G. Macromolecules 1989;22:4351.
[35] Mandelkern L, Alamo RG, Peña B. (in preparation).